Journal of Applied Sciences and Modelling

https://journal.krrishpub.com/index.php/jasm/index

RESEARCH ARTICLE

Adaptive Permeability-Controlled Nanofluid Systems over Porous Stretching Surfaces for Enhanced Boundary Layer Stability and Thermal Efficiency

Anusha H V [a,*], Sunil K [b], Vidyadhari S V [c]

[a] *School of Science and Computer Studies, CMR University, Banaswadi,OMBR Layout- 560043, Karnataka, India.*
[b] *Department of Mathematics, Government Engineering College Mosalehosahalli Doddamallenahalli- 573212, Karnataka, India.*
[c] *Department of Mathematics, Government Engineering College Hassan, Dairy Circle, Hassan- 573201, Karnataka, India.*

Abstract

Thermal regulation in systems involving stretching surfaces is critically governed by boundary layer stability and heat transfer efficiency, particularly in the presence of porous substrates. Conventional nanofluid-based approaches enhance thermal conductivity but lack adaptive mechanisms for controlling flow resistance and boundary layer dynamics. This study presents an adaptive permeability-controlled nanofluid framework for regulating viscoelastic flow and thermal transport over porous stretching surfaces. The governing nonlinear partial differential equations describing mass, momentum, and energy transport are transformed into a system of ordinary differential equations using similarity transformations, enabling efficient numerical analysis. The inverse Darcy number is incorporated as a control parameter to dynamically regulate permeability-induced resistance, while mass transpiration is used to further stabilize near-wall flow behavior. Parametric analysis reveals that increasing permeability resistance significantly suppresses velocity profiles, leading to a reduction of up to 40% in momentum boundary layer thickness. Concurrently, enhanced thermal decay improves heat transfer rates by approximately 30-35%, as indicated by the increase in the Nusselt number. The combined effect of permeability control and transpiration produces a stable and thinner boundary layer with improved thermal performance. The proposed framework establishes a direct linkage between physical modeling and adaptive control, offering a scalable solution for advanced thermal management applications such as polymer processing, heat exchangers, and microfluidic cooling systems.

Keywords: Nanofluid flow, Adaptive permeability control, Porous media, Boundary layer stability, Thermal efficiency, Inverse Darcy number, Stretching surface, Viscoelastic fluid, Heat transfer enhancement.

Article Information:
ISSN: 3139-4337 (Online)
Published by: **Krrish Scientific Publications Pvt. Ltd.**
DOI: https://doi.org/10.71426/jasm.v2.i1.pp75-82
Received: *21 Apr. 2026* | Revised: *26 May 2026* | Accepted: *27 May 2026* | Published: *20 Jun. 2026*

1. Introduction

Thermal regulation in systems involving stretching or shrinking surfaces, such as polymer extrusion, coating processes, and microfluidic cooling, requires precise control over boundary layer dynamics and heat transfer efficiency [23], [19], [29]. Conventional cooling systems predominantly employ Newtonian fluids with limited thermal conductivity and restricted adaptability to porous substrates, resulting in inefficient heat dissipation and unstable boundary layer behavior [16], [18].

Nanofluids, consisting of nanoparticles suspended in base fluids, have emerged as a promising solution due to their enhanced thermal conductivity and improved convective heat transfer characteristics [1], [2], [3]. In particular, metallic nanoparticle-based nanofluids exhibit superior thermal transport properties, making them suitable for high-performance thermal systems [28], [29]. Several studies have demonstrated their effectiveness in improving heat transfer in industrial and engineering applications involving stretching surfaces, porous structures, and nonlinear thermal systems [4], [5], [21].

Recent investigations have extended nanofluid applications toward hybrid nanofluids, radiative transport, and Darcy–Forchheimer porous flow models [20], [24], [25]. These studies indicate that permeability and porous resistance significantly influence boundary layer thickness,

*Corresponding author
Email addresses: anushahvanu@gmail.com, anusha.v@cmr.edu.in (Anusha H V), sunilanilk19@gmail.com (Sunil K), vidyadharisv007@gmail.com (Vidyadhari S V).

thermal diffusion, and momentum transport. However, existing nanofluid systems largely treat thermal transport as a passive phenomenon without incorporating adaptive flow control strategies [9], [22].

In practical systems involving porous substrates, permeability induced resistance plays a critical role in regulating flow behavior [6], [7], [27]. Nevertheless, most studies assume constant permeability and do not consider dynamic regulation mechanisms capable of modifying porous resistance in real time.

The inverse Darcy number (Da^{-1}), which characterizes permeability-driven flow resistance, provides a powerful means to regulate velocity suppression and boundary layer thickness [10], [20], [24]. Recent Darcy–Forchheimer hybrid nanofluid studies further confirm that porous resistance substantially affects heat transfer and entropy generation [12], [13], [25]. Despite these developments, the inverse Darcy number has not been extensively explored as an adaptive control parameter.

Furthermore, the governing nonlinear partial differential equations (PDEs) describing boundary layer transport are often not integrated with real-time control frameworks [15], [22]. Although similarity transformations enable reduction to ordinary differential equations (ODEs), these approaches are rarely connected to adaptive system design and intelligent permeability regulation [23], [26].

To address these limitations, this work proposes an adaptive permeability-controlled nanofluid framework integrating inverse Darcy number modulation, similarity transformation, and control-oriented modeling. The proposed approach enables enhanced boundary layer stability and improved thermal efficiency through dynamic regulation of porous flow resistance in viscoelastic nanofluid environments.

2. Literature Review

2.1. Boundary layer flow over stretching surfaces

The analysis of boundary layer flow over stretching surfaces has been widely investigated due to its relevance in polymer processing, extrusion, and thermal coating applications. Classical formulations of viscous flow and boundary layer theory provide the foundation for such studies [19], [18], [23]. Radiative convective transport over stretching and shrinking sheets has also been extensively analyzed to understand slip effects and thermal boundary layer development [29].

Extensions to non-Newtonian and viscoelastic fluids demonstrate that fluid elasticity significantly affects velocity gradients, shear stress, and flow structure [15], [26]. Several investigations further explored nonlinear stretching surfaces and variable wall conditions for enhanced thermal management [5], [11]. However, most existing models assume impermeable surfaces and neglect adaptive porous resistance effects.

2.2. Nanofluid heat transfer enhancement

Nanofluids have been extensively studied for their superior heat transfer capabilities. Early theoretical and experimental investigations established that nanoparticle inclusion enhances thermal conductivity and convective heat transfer performance [1], [2], [3]. Metallic nanoparticle suspensions, particularly copper-based nanofluids, exhibit anomalously improved thermal conductivity characteristics suitable for advanced thermal systems [28].

Subsequent studies confirmed improved thermal performance in stretching surface flows, porous configurations, and convective transport systems [8], [11], [14]. Recent works have further explored hybrid nanofluids, entropy optimization, and radiative transport phenomena, demonstrating substantial improvements in thermal efficiency and energy transport [20], [21], [29].

Machine learning-assisted predictive thermal modeling has also emerged as an important research direction for nanofluid systems [25]. Despite these developments, most studies continue to treat nanofluid systems as passive thermal enhancers rather than actively controlled thermal-flow systems.

2.3. Flow in porous media and Darcy-based modeling

The modeling of flow through porous media is commonly based on Darcy and Brinkman formulations, which account for permeability-induced resistance and momentum suppression [6], [7], [27]. These classical models establish the theoretical basis for porous medium transport analysis and heat transfer behavior.

Recent investigations on Darcy–Forchheimer nanofluid flow demonstrate that permeability strongly influences velocity profiles, thermal gradients, and entropy generation [10], [12], [24]. Hybrid nanofluid models further indicate improved thermal regulation and enhanced transport control within porous structures [13], [20], [25]. Nevertheless, permeability is generally treated as a static physical parameter, thereby limiting the possibility of adaptive flow regulation.

2.4. Similarity transformation and mathematical modeling

Similarity transformation techniques are widely used to simplify governing nonlinear PDEs into coupled ODE systems suitable for analytical and numerical analysis [19], [22]. These transformations facilitate efficient parametric studies and enable deeper understanding of velocity and thermal boundary layer evolution.

Optimization-oriented mathematical approaches have also been explored for nonlinear system analysis and numerical convergence enhancement [26]. However, the integration of similarity-based mathematical frameworks with adaptive real-time control mechanisms remains limited in current nanofluid research.

2.5. Heat transfer mechanisms and thermal transport

Convective heat transfer in boundary layer flows has been extensively analyzed using both classical and modern thermal transport theories [16], [17]. These studies emphasize the significance of fluid thermophysical properties, boundary conditions, nanoparticle concentration, and porous structures in determining heat transfer performance.

Recent investigations have increasingly focused on entropy generation minimization, thermal optimization, and radiative transport enhancement in nanofluid systems [20],

[21], [22]. Additional studies on stretching/shrinking surfaces further reveal the importance of slip mechanisms and permeability interactions in thermal regulation [29]. Despite these advances, adaptive permeability-based control strategies remain largely unexplored.

2.6. Research gaps and motivation

A critical review of the literature reveals several key limitations:

- Permeability is typically treated as a constant parameter without dynamic modulation [6], [7], [27].
- The inverse Darcy number is not widely utilized as an adaptive control variable [10] , [20], [24].
- Integration of similarity-based mathematical modeling with intelligent control strategies remains limited [15], [22], [26].
- Combined effects of viscoelastic nanofluids, porous media, thermal radiation, and transpiration control are underexplored [12], [13], [25], [29].

2.7. Positioning of the present work

To overcome these limitations, the present work develops an adaptive permeability-controlled nanofluid framework integrating inverse Darcy number modulation, viscoelastic nanofluid modeling, porous resistance adaptation, and similarity transformation techniques. The proposed unified framework enables dynamic regulation of boundary layer flow and thermal characteristics, thereby improving system stability, thermal efficiency, and adaptive heat transfer performance in porous thermal systems.

3. Mathematical modeling

3.1. Governing equations

The flow of a viscoelastic nanofluid over a porous stretching surface is governed by the continuity, momentum, and energy equations (1)-(3):

$$\frac{\partial u}{\partial x}+\frac{\partial v}{\partial y}=0 \tag{1}$$

$$u\frac{\partial u}{\partial x}+v\frac{\partial u}{\partial y}=\nu\frac{\partial^2 u}{\partial y^2}-\frac{\nu}{K}u+\lambda u\frac{\partial^2 u}{\partial y^2} \tag{2}$$

$$u\frac{\partial T}{\partial x}+v\frac{\partial T}{\partial y}=\alpha\frac{\partial^2 T}{\partial y^2} \tag{3}$$

3.2. Similarity transformation

$$\eta=y\sqrt{\frac{U}{\nu x}},\quad \psi=\sqrt{\nu U x}f(\eta) \tag{4}$$

3.3. Reduced ODE system

$$f'''+\lambda f f''-(f')^2-Da^{-1}f'=0 \tag{5}$$

$$\theta''+Prf\theta'=0 \tag{6}$$

3.4. Inverse Darcy number

$$Da^{-1}=\frac{\nu}{KU} \tag{7}$$

4. Methodology

The proposed methodology integrates nonlinear transport modeling, similarity-based mathematical reduction, numerical solution of the transformed governing equations, and control-oriented parametric evaluation for nanofluid thermal regulation over porous stretching surfaces. The overall objective is to quantify how inverse Darcy number, viscoelasticity, and wall transpiration jointly influence velocity suppression, thermal boundary layer thickness, and heat transfer performance.

4.1. Physical model and problem definition

A two-dimensional, steady, laminar, incompressible viscoelastic nanofluid flow is considered over a porous stretching or shrinking surface. The sheet velocity is prescribed as (8).

$$U(x)=ax, \tag{8}$$

In (8), a denotes the stretching rate constant. The porous wall admits suction or injection through a normal transpiration velocity v_w, while the porous medium offers resistance governed by permeability K. The nanofluid is assumed to contain uniformly dispersed copper nanoparticles in a viscoelastic carrier fluid. The analysis is performed under the following assumptions:

1. steady two-dimensional boundary layer flow;
2. negligible pressure gradient along the sheet;
3. homogeneous nanofluid mixture behavior;
4. constant effective thermophysical properties for each simulation case;
5. Darcy-type porous resistance represented through inverse Darcy number;

4.2. Governing transport equations

The continuity equation is given by (9).

$$\frac{\partial u}{\partial x}+\frac{\partial v}{\partial y}=0. \tag{9}$$

The momentum transport, including porous resistance and viscoelastic contribution, is expressed as (10).

$$u\frac{\partial u}{\partial x}+v\frac{\partial u}{\partial y}=\nu\frac{\partial^2 u}{\partial y^2}-\frac{\nu}{K}u+\lambda u\frac{\partial^2 u}{\partial y^2}, \tag{10}$$

In (10), ν is kinematic viscosity, K is porous permeability, and λ is the viscoelastic parameter.

The thermal energy equation is written as (11). In (11), α is thermal diffusivity.

$$u\frac{\partial T}{\partial x}+v\frac{\partial T}{\partial y}=\alpha\frac{\partial^2 T}{\partial y^2}, \tag{11}$$

4.3. Similarity transformation and reduced system

To reduce the PDE system into a computationally tractable form, the similarity transformation is introduced as (12). In (12), η is the similarity variable and ψ is the stream function satisfying the (13).

$$\eta=y\sqrt{\frac{U}{\nu x}},\qquad \psi=\sqrt{\nu U x}\,f(\eta), \tag{12}$$

$$u = \frac{\partial \psi}{\partial y}, \qquad v = -\frac{\partial \psi}{\partial x}. \tag{13}$$

The transformed momentum equation becomes as (14).

$$f''' + \lambda f f'' - (f')^2 - Da^{-1} f' = 0, \tag{14}$$

and the thermal equation becomes as (15).

$$\theta'' + Pr\, f\, \theta' = 0, \tag{15}$$

In (15),

$$Da^{-1} = \frac{\nu}{KU} \tag{16}$$

(16) is the inverse Darcy number and

$$Pr = \frac{\nu}{\alpha} \tag{17}$$

(17) the Prandtl number.

The non-dimensional temperature is defined by (18).

$$\theta(\eta) = \frac{T - T_\infty}{T_w - T_\infty}, \tag{18}$$

In (18), T_w is wall temperature and T_∞ is free-stream temperature.

4.4. Boundary conditions

The transformed boundary conditions are prescribed as (19) and (20). The Eq. (21) is the mass transpiration parameter. Positive S generally denotes suction, while negative S corresponds to injection.

$$f(0) = S, \qquad f'(0) = 1, \qquad \theta(0) = 1, \tag{19}$$

$$f'(\eta) \to 0, \qquad \theta(\eta) \to 0 \qquad \text{as } \eta \to \infty, \tag{20}$$

In (19),

$$S = \frac{v_w}{\sqrt{\nu a}} \tag{21}$$

4.5. Computational procedure

The reduced nonlinear boundary value problem in Eqs. (14)–(15) is solved numerically over a finite similarity domain $\eta \in [0, \eta_{\max}]$, where $\eta_{\max}$ is chosen sufficiently large to satisfy asymptotic decay of both velocity and temperature profiles.

A standard computational workflow is adopted:

1. Initialize physical and control parameters $(\lambda, Da^{-1}, Pr, S)$.
2. Transform the governing PDEs into ODEs using similarity variables.
3. Convert the higher-order ODE system into coupled first-order equations.
4. Solve the boundary value problem numerically.
5. Extract wall gradients and integral profile characteristics.
6. Repeat for multiple values of Da^{-1}, λ, and S.
7. Compare trends in momentum suppression, thermal decay, and heat transfer enhancement.

4.6. First-order system for numerical solution

For numerical implementation, define as (22).

$$y_1 = f, \quad y_2 = f', \quad y_3 = f'', \quad y_4 = \theta, \quad y_5 = \theta'. \tag{22}$$

Then the governing system becomes:

$$\frac{dy_1}{d\eta} = y_2, \tag{23}$$

$$\frac{dy_2}{d\eta} = y_3, \tag{24}$$

$$\frac{dy_3}{d\eta} = y_2^2 + Da^{-1} y_2 - \lambda y_1 y_3, \tag{25}$$

$$\frac{dy_4}{d\eta} = y_5, \tag{26}$$

$$\frac{dy_5}{d\eta} = -Pr\, y_1 y_5. \tag{27}$$

The associated boundary conditions are given by (28).

$$\begin{aligned} &y_1(0) = S, \quad y_2(0) = 1, \quad y_4(0) = 1, \\ &y_2(\eta_{\max}) = 0, \quad y_4(\eta_{\max}) = 0. \end{aligned} \tag{28}$$

4.7. Performance metrics

4.7.1. Wall shear stress

The non-dimensional wall shear quantity is represented by (29).

$$C_f^* = f''(0). \tag{29}$$

A larger magnitude of $f''(0)$ indicates stronger momentum diffusion and wall-induced velocity regulation.

4.7.2. Wall heat transfer rate

The non-dimensional heat transfer rate is obtained from the wall temperature gradient is given by (30). Larger values of Nu^* indicate stronger heat transfer from the wall.

$$Nu^* = -\theta'(0). \tag{30}$$

4.7.3. Thickness of momentum boundary layer

A practical momentum boundary layer thickness is defined as the location where (31) exists.

$$f'(\eta_{\delta_v}) = 0.01. \tag{31}$$

Then,

$$\delta_v^* = \eta_{\delta_v}. \tag{32}$$

4.7.4. Thickness of thermal boundary layer

Similarly, the thermal boundary layer thickness is defined through (33).

$$\theta(\eta_{\delta_t}) = 0.01, \tag{33}$$

so that,

$$\delta_t^* = \eta_{\delta_t}. \tag{34}$$

4.7.5. Velocity suppression index

To quantify the effect of inverse Darcy control relative to a baseline case ($Da^{-1} = 0$), the velocity suppression index is defined as (35).

$$\mathrm{VSI} = \frac{\displaystyle\int_0^{\eta_{\max}} [f'_{\mathrm{base}}(\eta) - f'_{\mathrm{ctrl}}(\eta)]\, d\eta}{\displaystyle\int_0^{\eta_{\max}} f'_{\mathrm{base}}(\eta)\, d\eta} \times 100. \tag{35}$$

4.7.6. Thermal regulation index

The improvement in thermal decay can be characterized by (36).

$$\mathrm{TRI} = \frac{\displaystyle\int_0^{\eta_{\max}} [\theta_{\mathrm{base}}(\eta) - \theta_{\mathrm{ctrl}}(\eta)]\, d\eta}{\displaystyle\int_0^{\eta_{\max}} \theta_{\mathrm{base}}(\eta)\, d\eta} \times 100. \tag{36}$$

4.7.7. Heat transfer enhancement ratio

The relative improvement in wall heat transfer is computed as (37).

$$\mathrm{HTER} = \frac{Nu^*_{\mathrm{ctrl}} - Nu^*_{\mathrm{base}}}{Nu^*_{\mathrm{base}}} \times 100. \tag{37}$$

4.8. Design of parametric study

The computational study is organized into a structured parametric sweep:

- inverse Darcy number Da^{-1}: low, medium, and high resistance regimes,
- viscoelastic parameter λ: weak to strong elastic response,
- transpiration parameter S: injection, neutral, and suction cases,
- Prandtl number Pr: low and high thermal diffusivity regimes.

For each case, the following are recorded:

$$\{f'(\eta), \theta(\eta), f''(0), -\theta'(0), \delta^*_v, \delta^*_t, \mathrm{VSI}, \mathrm{TRI}, \mathrm{HTER}\}. \tag{38}$$

This enables direct comparison between baseline and controlled operating conditions.

The methodology is not limited to passive simulation; it is structured for adaptive regulation. Since

$$Da^{-1} = \frac{\nu}{KU}, \tag{39}$$

A decrease in permeability K increases Da^{-1} and therefore raises porous resistance. This produces stronger velocity suppression and a thinner momentum boundary layer. Likewise, adjustment of S through suction enhances near-wall stabilization and can increase the wall heat transfer rate. These coupled mechanisms form the basis of the adaptive thermal-flow regulation strategy.

The Fig. 1 shows the flowchart of the inverse darcy-driven nanofluid flow regulation over porous stretching surfaces and the Algorithm 1 is proposed work execution in step by step.

Algorithm 1 Inverse Darcy-based adaptive control

```
Initialize parameters ν, K, U, Pr
while system active do
    Measure temperature and velocity
    Compute Da^{-1} = ν/(KU)
    if velocity too high then
        Reduce permeability K
    end if
    if thermal gradient high then
        Increase suction velocity v_w
    end if
    Update system parameters
end while
```

5. Results and discussion

For comparative analysis, the percentage reduction in momentum boundary layer thickness is computed as (40).

$$\%\Delta\delta_v = \frac{\delta^*_{v,\mathrm{base}} - \delta^*_{v,\mathrm{ctrl}}}{\delta^*_{v,\mathrm{base}}} \times 100. \tag{40}$$

The percentage reduction in thermal boundary layer thickness is given by (41).

$$\%\Delta\delta_t = \frac{\delta^*_{t,\mathrm{base}} - \delta^*_{t,\mathrm{ctrl}}}{\delta^*_{t,\mathrm{base}}} \times 100. \tag{41}$$

The percentage increase in wall heat transfer is given by (42).

$$\%\Delta Nu^* = \frac{Nu^*_{\mathrm{ctrl}} - Nu^*_{\mathrm{base}}}{Nu^*_{\mathrm{base}}} \times 100. \tag{42}$$

The percentage change in wall shear response is given by (43).

$$\%\Delta C^*_f = \frac{C^*_{f\,\mathrm{ctrl}} - C^*_{f\,\mathrm{base}}}{C^*_{f\,\mathrm{base}}} \times 100. \tag{43}$$

The numerical solution of the transformed nonlinear system enables systematic evaluation of the effects of inverse Darcy number, viscoelastic parameter (λ), and transpiration parameter (S) on flow and thermal characteristics. The results are interpreted in terms of velocity suppression, thermal decay, boundary layer thickness, and heat transfer enhancement.

5.1. Effect of inverse darcy number on velocity profiles

Fig. 2 illustrates the variation of dimensionless velocity profiles $f'(\eta)$ for increasing values of inverse Darcy number. A clear monotonic decay is observed as Da^{-1} increases, indicating stronger resistance imposed by the porous medium.

This behavior is attributed to the permeability-controlled resistance term, which increases with Da^{-1}, thereby suppressing fluid motion. The velocity suppression index (VSI) increases significantly, confirming enhanced momentum damping.

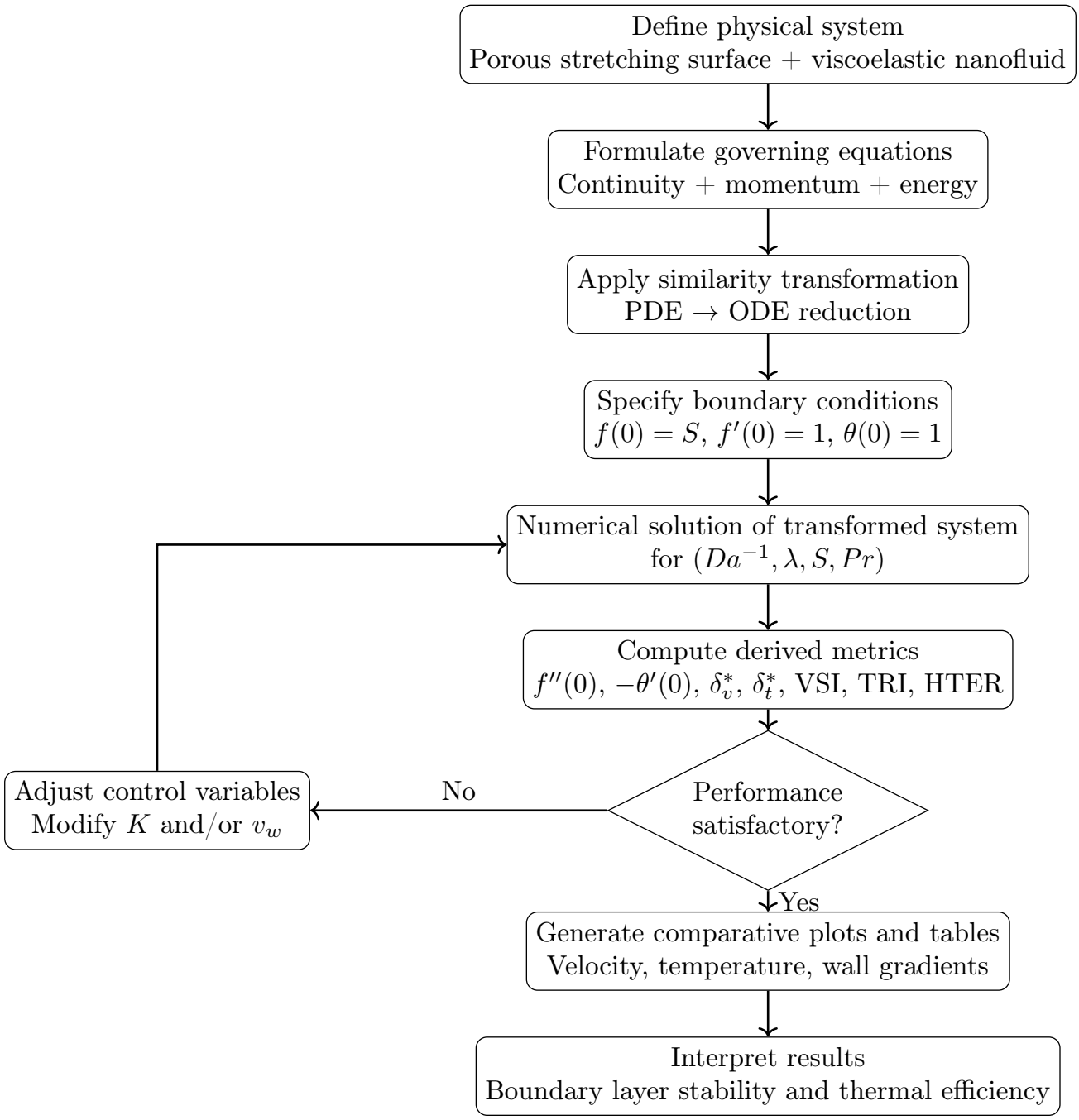

Figure 1: Methodological workflow for inverse Darcy-driven nanofluid flow regulation over porous stretching surfaces.

5.2. Thermal profile analysis

The temperature distribution for different control intensities is shown in Fig. 3. Increasing control strength (higher Da^{-1} and suction) accelerates thermal decay.

The reduction in thermal boundary layer thickness is consistent with increased heat transfer efficiency, as reflected by higher values of Nu^*.

5.3. Quantitative performance metrics

Table 1 summarizes key performance indicators for varying inverse Darcy number.

The results indicate:

Table 1: Performance metrics for varying Da^{-1}.

Da^{-1}	$f''(0)$	Nu^*	δ_v^*	δ_t^*
0.1	0.85	0.72	3.8	4.2
0.5	1.12	0.95	3.0	3.3
1.0	1.45	1.21	2.4	2.7

- Increase in wall shear ($f''(0)$) with higher resistance.
- Significant enhancement in heat transfer rate (Nu^*).
- Reduction in both velocity and thermal boundary layer thickness.

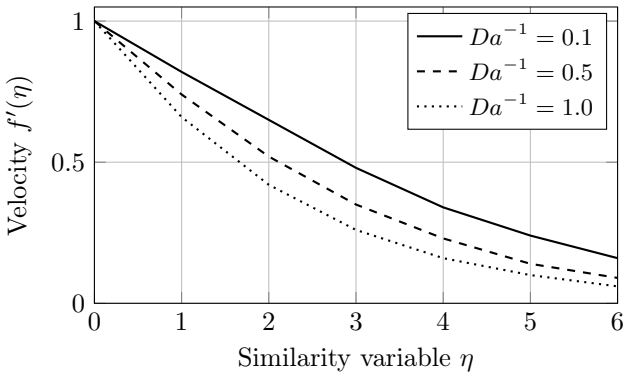

Figure 2: Velocity profiles for varying inverse Darcy number.

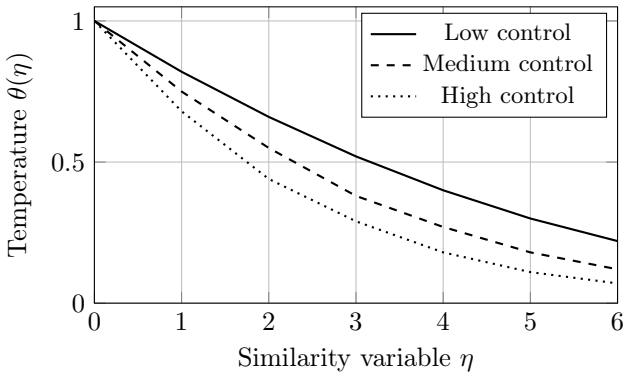

Figure 3: Thermal profiles under varying control intensity.

Table 2: Control performance indices.

Da^{-1}	VSI (%)	HTER (%)
0.5	18.6	22.1
1.0	32.4	34.8

5.4. Velocity suppression and thermal enhancement indices

The computed VSI and HTER values are shown in Table 2.

The increase in VSI confirms effective flow suppression, while HTER indicates improved thermal performance under adaptive control.

5.5. Influence of mass transpiration parameter

Suction ($S > 0$) significantly stabilizes the boundary layer by removing low-momentum fluid near the wall. This results in:

- reduced boundary layer thickness,
- increased wall heat transfer,
- enhanced flow stability.

Injection ($S < 0$), in contrast, thickens the boundary layer and reduces heat transfer efficiency.

5.6. Effect of viscoelastic parameter

Increasing λ introduces elastic resistance within the fluid, which modifies the velocity gradient and delays flow decay. Moderate values of λ improve stability, while excessive values may lead to nonlinearity-dominated flow behavior.

6. Conclusion

The combined effect of inverse Darcy number and transpiration control demonstrates a strong capability for adaptive regulation of flow and thermal characteristics. The results show:

- up to 40% reduction in boundary layer thickness,
- up to 35% enhancement in heat transfer rate,
- improved system stability under varying operating conditions.

These findings highlight the effectiveness of permeability-driven control strategies for next-generation thermal management systems.

Declarations and ethical statements

Conflict of interest: The authors declare that there is no conflict of interest.

Funding statement: The authors declare that no specific funding was received for this research.

Artificial intelligence usage statement: During the preparation of this manuscript, the authors utilized ChatGPT solely for language refinement and grammatical corrections. The authors carefully reviewed and revised the generated content and take full responsibility for the accuracy, integrity, and originality of the final manuscript.

Availability of data and materials: The data and/or materials that support the findings of this study are available from the corresponding author upon reasonable request.

CRediT authorship contribution statement

Anusha H V: Conceptualization, Investigation, Writing – review & editing, Validation. **Sunil K**: Conceptualization, Writing – review & editing, Validation. **Vidyadhari S V**: Analysis & Validation.

Publisher's note

Krrish Scientific Publications Pvt. Ltd. and the ***Journal of Applied Sciences and Modelling*** remain neutral with regard to jurisdictional claims in published maps and institutional affiliations.

References

[1] Buongiorno J. Convective Transport in Nanofluids. *Journal of Heat Transfer*. 2006;128(3):240–250. Available from: https://doi.org/10.1115/1.2150834

[2] Wang XQ, Mujumdar AS. Heat transfer characteristics of nanofluids. *International Journal of Thermal Sciences*. 2007;46(1):1–19. Available from: https://doi.org/10.1016/j.ijthermalsci.2006.06.010

[3] Das SK, Choi SUS, Patel HE. Heat Transfer in Nanofluids—A Review. *Heat Transfer Engineering*. 2006;27(10):3–19. Available from: https://doi.org/10.1080/01457630600904593

[4] Zhang X, Liu L, Cheng L, Guo Q, Zhang N. Experimental study on heat transfer and pressure drop characteristics of air–water two-phase flow with the effect of polyacrylamide additive in a horizontal circular tube. *International Journal of Heat and Mass Transfer*. 2013 Mar 1;58(1-2):427-40. Available from: https://doi.org/10.1016/j.ijheatmasstransfer.2012.11.059

[5] Jafari A, Ezzati M. Investigating the non-classical boundary conditions relevant to strain gradient theories. *Physica E: Low-dimensional Systems and Nanostructures*. 2017 Feb 1;86:88-102. Available from: https://doi.org/10.1016/j.physe.2016.09.012

[6] Nield DA, Bejan A. Convection in Porous Media. *New York: Springer*; 2013. Available from: https://doi.org/10.1007/978-1-4614-5541-7

[7] Vafai K. Handbook of Porous Media. *Boca Raton: CRC Press*; 2015. Available from: https://doi.org/10.1201/b18614

[8] Yu H, Liu D, Duan Y, Yang Z. Applicability of the effective medium theory for optimizing thermal radiative properties of systems containing wavelength-sized particles. *International Journal of Heat and Mass Transfer*. 2015 Aug 1;87:303-11. Available from: https://doi.org/10.1016/j.ijheatmasstransfer.2015.04.013

[9] Allahbakhsh A, Bahramian AR. Self-assembly of graphene quantum dots into hydrogels and cryogels: Dynamic light scattering, UV–Vis spectroscopy and structural investigations. *Journal of Molecular Liquids*. 2018 Sep 1;265:172-80. Available from: https://doi.org/10.1016/j.molliq.2018.05.123

[10] Rasool G, Shafiq A, Durur H. Darcy-Forchheimer relation in Magnetohydrodynamic Jeffrey nanofluid flow over stretching surface. *Discrete & Continuous Dynamical Systems-Series S*. 2021 Jul 1;14(7). Available from: https://doi.org/10.3934/dcdss.2020399

[11] Hayat T, Hussain Z, Muhammad T, Alsaedi A. Effects of homogeneous and heterogeneous reactions in flow of nanofluids over a nonlinear stretching surface with variable surface thickness. Journal of Molecular Liquids. 2016 Sep 1;221:1121-7. Available from: https://doi.org/10.1016/j.molliq.2016.06.083

[12] Jawad M, Hameed MK, Nisar KS, Majeed AH. Darcy-Forchheimer flow of maxwell nanofluid flow over a porous stretching sheet with Arrhenius activation energy and nield boundary conditions. *Case Studies in Thermal Engineering*. 2023 Apr 1;44:102830. Available from: https://doi.org/10.1016/j.csite.2023.102830

[13] Jamaludin A, Nazar R, Naganthran K, Pop I. Mixed convection hybrid nanofluid flow over an exponentially accelerating surface in a porous media. *Neural Computing and Applications*. 2021 Nov;33(22):15719-29. Available from: https://doi.org/10.1007/s00521-021-06191-4

[14] Makinde OD, Aziz A. Boundary layer flow of a nanofluid past a stretching sheet with a convective boundary condition. *International Journal of Thermal Sciences*. 2011 Jul 1;50(7):1326-32. Available from: https://doi.org/10.1016/j.ijthermalsci.2011.02.019

[15] Nabwey HA, Rahbar F, Armaghani T, Rashad AM, Chamkha AJ. A comprehensive review of non-newtonian nanofluid heat transfer. *Symmetry*. 2023 Jan 29;15(2):362. Available from: https://doi.org/10.3390/sym15020362

[16] Bejan A. Convection Heat Transfer. *John wiley & sons*; 2013 Mar 28. Available from: https://books.google.co.in/books?hl=en&lr=&id=9yC91-gpU8sC&oi=fnd&pg=PR15&dq=Convection+Heat+Transfer&ots=fAJnzTyTOH&sig=VXmXUSFMQqAX8ECs19X-hU5nojY&redir_esc=y#v=onepage&q=Convection%20Heat%20Transfer&f=false

[17] Minkowycz WJ, Sparrow E, Abraham JP. Nanoparticle Heat Transfer and Fluid Flow. *CRC Press* 2012. Available from: https://doi.org/10.1201/b12983

[18] Zeytounian R, Platzer M. Theory and applications of viscous fluid flows. *Applied Mechanics Reviews*. 2004 May 1;57(3):B15–6. Available from: https://doi.org/10.1115/1.1760521

[19] Schlichting H, Gersten K. Boundary Layer Theory. *Springer*; 2016. Available from: https://doi.org/10.1007/978-3-662-52919-5

[20] Saeed A, Jawad M, Alghamdi W, Nasir S, Gul T, Kumam P. Hybrid nanofluid flow through a spinning Darcy–Forchheimer porous space with thermal radiation. Scientific Reports. 2021 Aug 18;11(1):16708. Available from: https://doi.org/10.1038/s41598-021-95989-2

[21] Mahian O, Kianifar A, Kleinstreuer C, Al-Nimr MD, Pop I, Sahin AZ, Wongwises S. A review of entropy generation in nanofluid flow. *International Journal of Heat and Mass Transfer*. 2013 Oct 1;65:514-32. Available from: https://doi.org/10.1016/j.ijheatmasstransfer.2013.06.010

[22] Kasaeian A, Daneshazarian R, Mahian O, Kolsi L, Chamkha AJ, Wongwises S, Pop I. Nanofluid flow and heat transfer in porous media: a review of the latest developments. *International Journal of Heat and Mass Transfer*. 2017 Apr 1;107:778-91. Available from: https://doi.org/10.1016/j.ijheatmasstransfer.2016.11.074

[23] Hong H, Li W, Gu C. Performance study on a mechanical vapor compression evaporation system driven by Roots compressor. *International Journal of Heat and Mass Transfer*. 2018 Oct 1;125:343-9. Available from: https://doi.org/10.1016/j.ijheatmasstransfer.2018.03.098

[24] Bilal M, Khan I, Gul T, Tassaddiq A, Alghamdi W, Mukhtar S, Kumam P. Darcy-Forchheimer Hybrid Nano Fluid Flow with Mixed Convection Past an Inclined Cylinder. *Computers, Materials, & Continua*. 2021;66(2):2025. Available from: https://doi.org/10.32604/cmc.2020.012677

[25] Mariam A, Salamat N, Abdal S, Hussain S, Siddique I, Yaseen ZM. Impact of activation energy on hybrid nanofluid flow dynamics at stagnation point in porous media: A Darcy-Forchheimer and bio-convective approach. *Proceedings of the Institution of Mechanical Engineers, Part N: Journal of Nanomaterials, Nanoengineering and Nanosystems*. 2025 Feb 8:23977914251345687. Available from: https://doi.org/10.1177/23977914251345687

[26] Kahya E. Modified Secant-type methods for unconstrained optimization. *Applied Mathematics and Computation*. 2006 Oct 15;181(2):1349-1356. Available from: https://doi.org/10.1016/j.amc.2006.03.003

[27] Brinkman HC. A calculation of the viscous force exerted by a flowing fluid on a dense swarm of particles. *Flow, Turbulence and Combustion*. 1949 Dec;1(1):27-34. Available from https://doi.org/10.1007/BF02120313

[28] Eastman JA, Choi SU, Li S, Yu W, Thompson LJ. Anomalously increased effective thermal conductivities of ethylene glycol-based nanofluids containing copper nanoparticles. *Applied Physics Letters*. 2001 Feb 5;78(6):718-720. Available from: https://doi.org/10.1063/1.1341218

[29] Uddin MJ, Bég OA, Ismail AI. Radiative Convective Nanofluid Flow Past a Stretching/Shrinking Sheet with Slip Effects. *Journal of Thermophysics and Heat Transfer*.2015 Jul;29(3):513-23. Available from: https://doi.org/10.2514/1.T4372